Available online at www.sciencedirect.com
ScienceDirect
Trans. Nonferrous Met. Soc. China 24(2014) 930−939
Transactions of Nonferrous Metals Society of China
www.tnmsc.cn

Flow behavior and microstructure of ZK60 magnesium alloy compressed at high strain rate

Yuan-zhi WU[1,2], Hong-ge YAN[3], Su-qin ZHU[4], Ji-hua CHEN[3], An-min LIU[1,2], Xian-lan LIU[1]

1. Department of Mechanical Engineering, Hunan Institute of Technology, Hengyang 421002, China;
2. Institute of Advance Manufacturing Technology, Hunan Institute of Technology, Hengyang 421002, China;
3. College of Materials Science and Engineering, Hunan University, Changsha 410082, China;
4. School of Aerospace, Mechanical & Mechatronic Engineering, The University of Sydney, Sydney NSW 2006, Australia

Received 8 May 2013; accepted 26 August 2013

Abstract: Flow behavior and microstructure of a homogenized ZK60 magnesium alloy were investigated during compression in the temperature range of 250−400 °C and the strain rate range of 0.1−50 s^{-1}. The results showed that dynamic recrystallization (DRX) developed mainly at grain boundaries at lower strain rate (0.1−1 s^{-1}), while in the case of higher strain rate (10−50 s^{-1}), DRX occurred extensively both at twins and grain boundaries at all temperature range, especially at temperature lower than 350 °C, which resulted in a more homogeneous microstructure than that under other deformation conditions. The DRX extent determines the hot workability of the workpiece, therefore, hot deformation at the strain rate of 10−50 s^{-1} and in the temperature range of 250−350 °C was desirable for ZK60 alloy. Twin induced DRX during high strain rate compression included three steps. Firstly, twins with high dislocation subdivided the initial grain, then dislocation arrays subdivided the twins into subgrains, and after that DRX took place with a further increase of strain.

Key words: ZK60 magnesium alloy; high strain rate compression; flow behavior; microstructure; twin induced DRX

1 Introduction

Magnesium alloys hold great potential for energy saving and carbon emission reduction from aeroplane and automobile industry due to a combination of reduced mass, improved machinability, excellent damping capacity and recycling capability [1,2]. Presently, most parts made from magnesium alloys are manufactured by the die casting process. However, the cast products have poor mechanical strength because of the casting defects such as porosity and segregation, which limit the widespread application of magnesium alloys [3,4]. Compared with cast magnesium alloys, wrought magnesium alloys have attracted increasing interests due to their higher mechanical strength and better ductility. ZK60 alloy is a typical high-strength wrought magnesium alloy which has been characterized by good stress corrosion resistance and heat treatability [5,6]. However, owing to the limited slip systems in the hexagonal close-packed (HCP) lattice, plastic deformation of magnesium at room temperature is difficult. Therefore, it is necessary for magnesium alloys to deform at warm temperatures (>225 °C), at which the non-basal slip systems can be activated [7]. In order to optimize the hot processing parameters of ZK60 alloys, it is important to understand the effect of temperature and strain rate on flow behavior and microstructure of the alloys. Therefore, investigation on the hot deformation behavior of ZK60 alloy has attracted more and more attention in recent years [8−13]. However, most of them were conducted at strain rate lower than 10 s^{-1} [8−12], and only a few studies were operated at strain rate higher than 10 s^{-1} [13], where the plastic deformation may be performed. The absence of the related data on the forming technological factors is still existent, which limits the widespread use of ZK60 alloy.

In this work, flow stress and microstructure of

Foundation item: Project (14JJ6047) supported by the Natural Science Foundation of Hunan Province, China; Project (51274092) supported by the National Natural Science Foundation of China; Project (20120161110040) supported by the Doctoral Program of Higher Education of China

Corresponding author: Yuan-zhi WU; Tel: +86-734-3452089; E-mail: yzwu666@gmail.com

DOI: 10.1016/S1003-6326(14)63145-9

homogenized ZK60 magnesium alloys during high strain rate compression was investigated to provide a useful guide for the selection of the hot working processing (including forging and rolling) parameters.

2 Experimental

Hot compression tests were conducted on a commercial ZK60 alloy produced by semi-continuous cast supplied by Winca Corporation with the chemical compositions of Mg−5.5Zn−0.45Zr (mass fraction, %). The as-cast billets were homogenized at 330 °C for 30 h followed by water quenching. Cylindrical specimens with the diameter of 10 mm and the height of 15 mm were machined from the homogenized billets and both ends of each specimen were recessed to the depth of 0.2 mm to entrap the lubricant.

Compression tests were carried out using a computer servo-controlled Gleeble 1500 machine in the strain rate range of 0.1−50 s^{-1} and the deformation temperature range of 250−400 °C with a reduction ranging from 10% to 50%. The machine oil mixed with the graphite powders was used as the lubricant at the interface between the anvil and the specimen. Specimens were heated to the set temperature at a rate of 200 °C/min and held for 3 min before compression. The specimens were then water quenched immediately after compression. No obvious cracks were observed on all the hot-compressed specimens. The deformed microstructures perpendicular to the deformation axis were observed by optical microscope (OM) and transmission electron microscope (TEM).

3 Results and discussion

3.1 Flow behavior

The true stress–true strain curves of the homogenized ZK60 alloy hot compressed at various strain rates and temperatures are shown in Fig. 1. At the strain rate lower than 1 s^{-1}, the curves were characteristic of initial work hardening followed by the flow softening. At the strain rate higher than 10 s^{-1}, work hardening was more rapid and discontinuous yielding occurred at the true strain less than 0.05 and then continuous softening appeared after the peak stress with the strain increasing, and the flow softening extents were more pronounced for samples compressed at higher strain rates (≥10 s^{-1}) than lower strain rates (≤1 s^{-1}). Flow softening could be ascribed to the dynamic recrystallization (DRX), the dynamic recovery (DRV), the temperature rise of the specimen and grain coarsening during hot compression [14]. Therefore, it is difficult to determine the optimum hot working processing only according to the shape of the true stress–true strain curves.

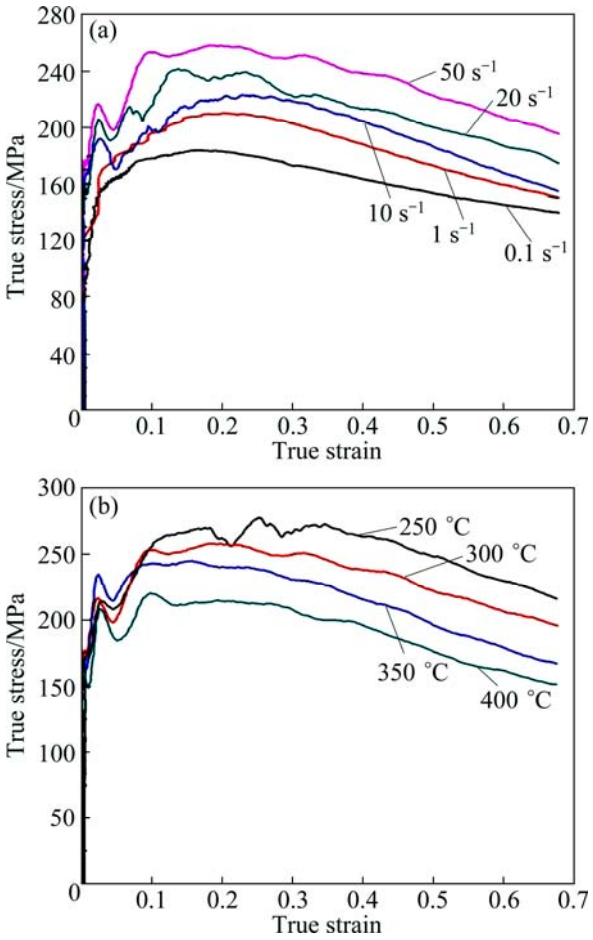

Fig. 1 True stress−true strain curves of ZK60 hot compressed at different conditions: (a) At 300 °C for various strain rates; (b) With strain rate 50 s^{-1} at various temperatures

The flow stress of ZK60 increased with the increase of the strain rate at certain temperature since the increase in the strain rate led to a higher dislocation density. On the other hand, the flow stress decreased with the increase of temperature at a fixed strain rate. It could be ascribed to the reduced critical resolved shear stress for the non-basal slip at a higher temperature and the more readily operable non-basal slip at a higher deformation temperature.

3.2 Microstructures

The microstructures of the as-cast and homogenized ZK60 magnesium alloys are shown in Figs. 2(a) and (b), respectively. As seen from Fig. 2(a), the as-cast microstructure consisted of uneven α-Mg matrix and discontinuous distributed eutectic compounds at the grain boundaries. After it was homogenized, the alloy had an average grain size of ~100 μm and few eutectic compounds distributed at grain boundaries, as shown in

Fig. 2(b). For the present samples with coarse-grain microstructures, grain boundary sliding could hardly be expected to play an important role in plastic deformation. The deformation behavior was likely to be implemented by other mechanisms such as twinning and DRX, which was clarified by the microstructure observation in this study.

Microstructures of the samples compressed to a true strain of 0.69 at the strain rate of 0.1 s^{-1} are shown in Figs. 3(a) and (b). The as-compressed microstructures were composed of twins in the grain interior and DRX grains at grain boundaries. Even necklace DRX grains at grain boundaries and twins inside the initial grains were observed at 250 °C. With increasing the temperature, owing to the operation of non-basal slip, fewer twins and more DRX grains were formed in the grain interior and along grain boundaries, respectively. Almost no twins were observed with the hot compression temperature up to 350 °C. As indicated in Figs. 3(c) and (d), the microstructure evolution of the as-compressed samples at the strain rate of 1 s^{-1} was similar to that at the strain rate of 0.1 s^{-1}, but twinning was more extensively with the strain rate increasing to 1 s^{-1}at 250 °C.

Because of the HCP lattice and limited slip system, twinning plays a significant role in magnesium deformation at low temperature to help this material to satisfy the von Mises criterion, which requires five independent deformation systems for an arbitrary

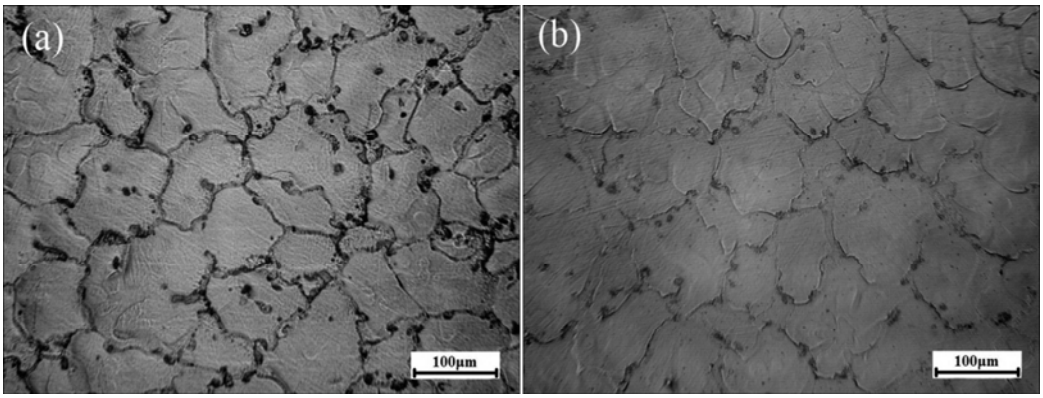

Fig. 2 OM images of ZK60 magnesium alloy in as-cast (a), homogenized (b) states

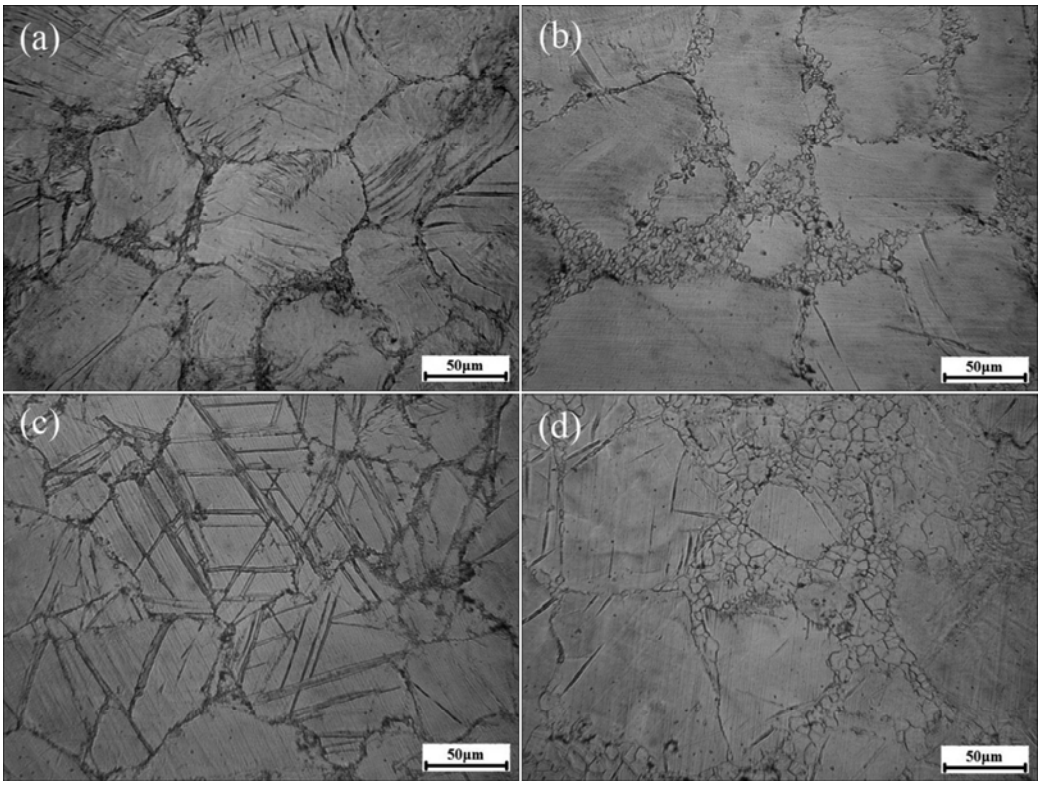

Fig. 3 OM images of ZK60 compressed to strain of 0.69 at different conditions: (a) 250 °C, 0.1 s^{-1}; (b) 350 °C, 0.1 s^{-1}; (c) 250 °C, 1 s^{-1}; (d) 350 °C, 1 s^{-1}

homogeneous straining. Twinning was reported to be the main mechanism for ZK21 alloy deformed at low temperatures (250−300 °C) and low strain rates (≤1 s^{-1}) in the previous work [15], and almost no DRX grain can be observed. Different from ZK21 alloy, DRX developed extensively at grain boundaries associated with fewer twins in ZK60 alloy deformed at the same conditions as seen from Figs. 1(a) and (c). Higher Zn content in ZK60 alloy may make the difference ascribe to the following factors. Firstly, the solid solution atom of Zn plays more significant role in dragging dislocation. Secondly, the precipitated second phase formed during hot deformation should block the movement of dislocation. Thirdly, lower stacking fault energy (SFE) reduces the tendency for dislocation pile-up to cross-slip [9,16]. As temperature increases, few twins were formed due to the operation of the non-basal slip and necklace DRX microstructure was formed. The necklace DRX occurred in other magnesium alloys during compression and the mechanism was reported in Refs. [17,18]. DRX sets in the position where the high misorientations are created by the accumulation of dislocations, i.e., grain boundaries. Later, new fine grains are formed as a necklace along grain boundaries. As shown in Figs. 3(b) and (d), DRX at the grain boundaries was the dominant deformation mechanism for ZK60 deformed at the higher temperature (350−400 °C) and the lower strain rate (≤1 s^{-1}). In the correlation with Fig. 1, DRX at the grain boundaries was ascribed to the flow softening.

As seen from Fig. 4, the microstructures of the sample compressed at the strain rate of 10 s^{-1} were obviously different from those at lower strain rates (≤1 s^{-1}). Moreover, more twins were observed with the increasing strain rate, which can be seen even at high temperatures, although the twin density decreased with the increase of temperature, and DRX developed both at initial grain boundaries and twins. Microstructures of the samples compressed to a true strain of 0.69 at the strain rate of 20 s^{-1} and 50 s^{-1} are shown in Fig. 5. Twins were observed in the samples at all the temperatures and the DRX was more extensive than that at the lower strain rates. The DRX grains were observed both at the grain boundaries and twins, and fewer twins were formed with the temperature increasing. In the combination with Figs. 5(c) and (d), the microstructure evolution of the as-compressed samples at the strain rate of 20 s^{-1} or 50 s^{-1} with the temperature increasing was similar to that at the strain rate of 10 s^{-1}. Therefore, DRX developed extensively at the grain boundaries and twins was the main deformation mechanism at all the temperature ranges (250−400 °C) and the higher strain rate (≥10 s^{-1}), resulting in a more homogeneous microstructure. In the correlation with Fig. 1, twinning was thus ascribed to the high strain hardening rate of the specimens deformed at

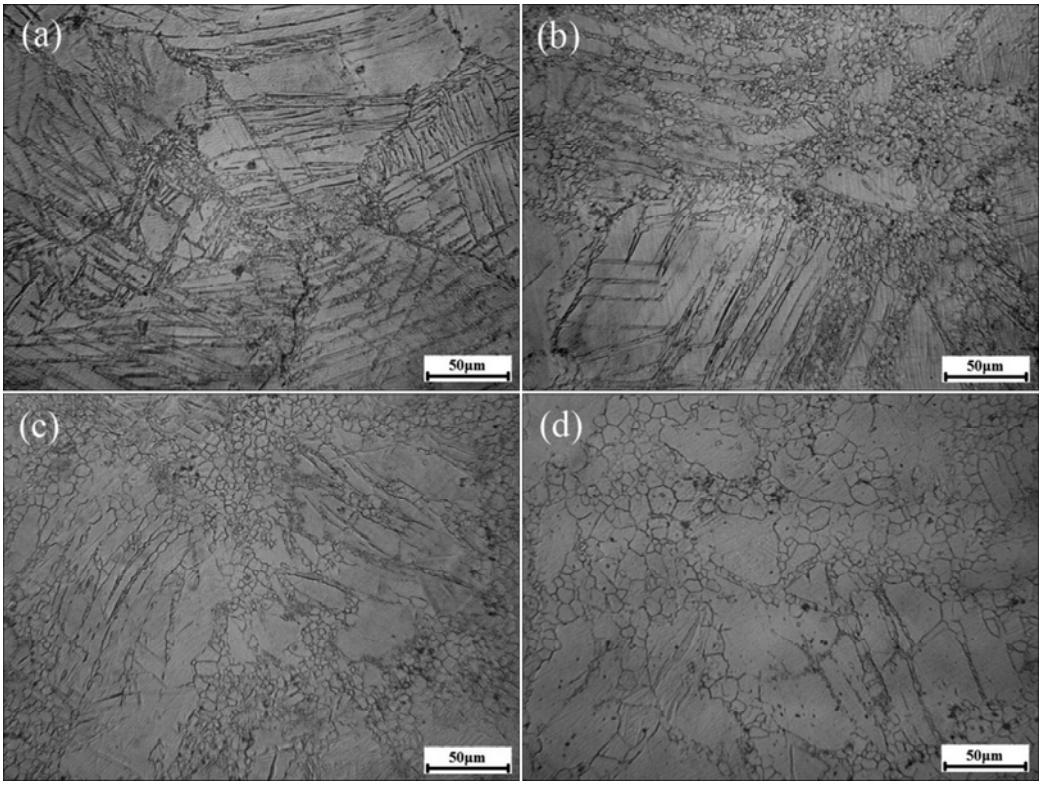

Fig. 4 OM images of ZK60 compressed to strain of 0.69 at different temperatures with strain rate of 10 s^{-1}: (a) 250 °C; (b) 300 °C; (c) 350 °C; (d) 400 °C

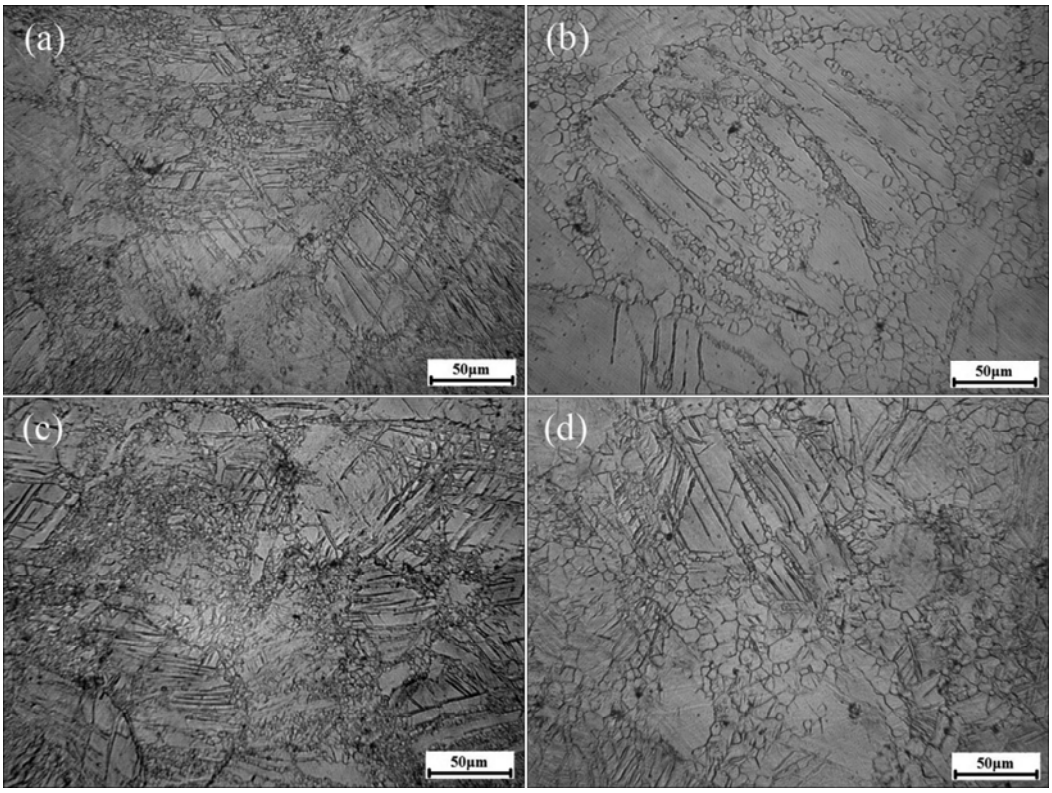

Fig. 5 OM images of ZK60 compressed to strain of 0.69 at different conditions: (a) 250 °C, 20 s^{-1}; (b) 400 °C, 20 s^{-1}; (c) 250 °C, 50 s^{-1}; (d) 400 °C, 50 s^{-1}

higher strain rate, and a large content of DRX probably resulted in the evident flow softening at higher strain rate deformation.

During the high-strain rate deformation, there was limited time for the movement of dislocation and thus a large number of twins were formed to accommodate the deformation process even at the higher temperatures, which was similar to the high strain rate deformation behavior of ZK21 and ZK40 alloys [15,19]. DRX occurred both at grain boundaries and twins. However, the twin boundary plays a more significant role than the grain boundary in the samples deformed at the higher strain rate. Therefore, the DRX development was controlled by the formation of DRX grains at the twins in ZK60 alloys during high strain rate hot compression.

The large DRX extent is chosen for the hot working of materials since this process yields good workability and microstructure free from failure [20]. In this study, DRX occurred mainly at grain boundaries and twins, and thus the DRX extent at grain boundaries and twins played determinant role in the hot workability of ZK60. For the samples compressed at the lower strain rate (≤1 s^{-1}), DRX was developed at grain boundaries, resulting in the necklace DRX grains. At the higher-strain rate(≥10 s^{-1}), a large number of twins were generated due to the high strain rate deformation and DRX was extensively developed at the grain boundaries and twins especially at temperature lower than 350 °C, resulting in a more homogeneous microstructure. Therefore, hot deformation at the strain rate of 10−50 s^{-1} in the temperature range of 250−350 °C was desirable and feasible for the ZK60 alloys. Obviously, twin induced DRX plays an important role in the high-strain rate deformation and the DRX mechanism is worthy of further research.

The micrographs of ZK60 alloys compressed at strain rate of 20 s^{-1} under 300 °C with different reduction amounts were shown in Fig. 6. Twins with high dislocation density were observed and divided the initial grain into fine twin lamellas at the initial stage of high-strain rate compression as seen in Figs. 6(a) and (b), which imply that the twin boundaries should pile up dislocations as grain boundaries. The twin density increased with increasing strain and DRX took place at some twins as illustrated in Fig. 6(c), meanwhile, the dislocation arrays subdivided the un-DRX twins into subgrains with storage of high strain energy as shown in Fig. 6(d). With a further increasing in strain, DRX took place at twin extensively and the subgrains with high dislocation density were replaced by DRX grain with rather low dislocation density as shown in Figs. 6(e) and (f). As indicated in Figs. 6(b), (d) and (f), the twin induced DRX during high-strain rate compression of

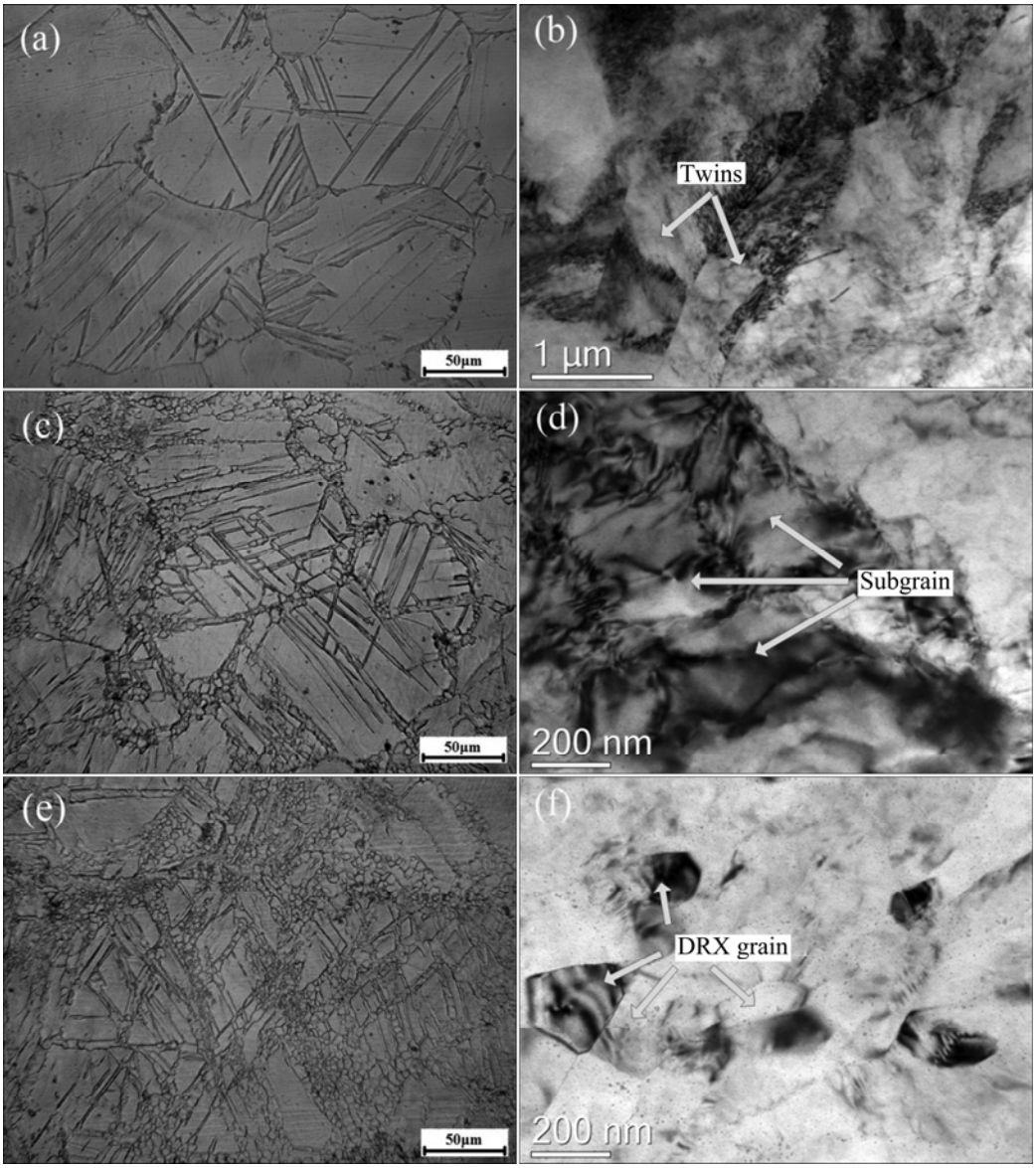

Fig. 6 OM (a, c, e) and TEM (b, d, f) images of ZK60 compressed at strain rate of 20 s^{-1} under 300 °C with reduction amounts of 10% (a, b), 30% (c, d) and 50% (e, f)

ZK60 alloy was consistent with that of AZ91 alloy deformed at rather high strain in Ref. [21]. Twins were extensively developed at initial grain, and then dislocation arrays subdivided the twins into subgrains, after that DRX took place with a further increase in strain.

3.3 Constitutive analysis

During hot working, three constitutive equations have been proposed to describe the hot deformation behaviors of metals [22]:

$$\dot{\varepsilon} = A_1\sigma^{n_1}\exp\left(\frac{-Q}{RT}\right) \quad (1)$$

$$\dot{\varepsilon} = A_2\exp(\beta\sigma)\exp\left(\frac{-Q}{RT}\right) \quad (2)$$

$$\dot{\varepsilon} = A[\sinh(\alpha\sigma)]^n\exp\left(\frac{-Q}{RT}\right) \quad (3)$$

where A, A_1, A_2, n, n_1, α and β are constants; Q is the activation energy for deformation; R is the gas constant. The value of the constant α can be deduced by the division result of β and n_1 which are material constants of the two conventional equations, i.e., the exponential law (Eq. (2)) and the power law (Eq. (1)).

Utilizing the experimental data, the plots that describe the relationship between steady state stress and strain rate according to the power law and exponential law are given in Figs. 7 (a) and (b), respectively. Based on the best-fitting lines in the plots, the values of n_1 and β are deduced to be 15.41 and 0.074, respectively. Thus the value of α is calculated to be 0.005 MPa^{-1}.

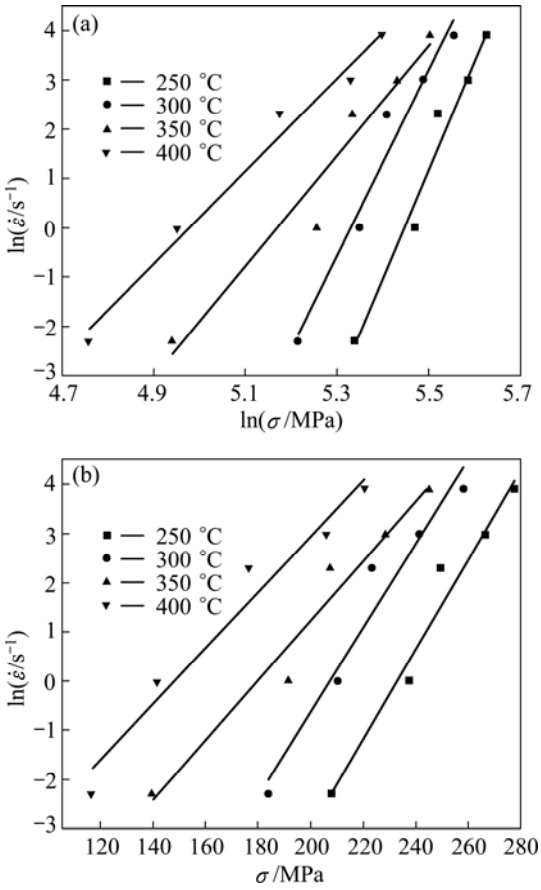

Fig. 7 Relationship between steady state stress and strain rate according to power law (a), and exponential law (b)

The hot deformation conditions are usually expressed in terms of temperature compensated strain rate, namely the Zener−Hollomon (Z) parameter [22]:

$$Z = \dot{\varepsilon}\exp\left(\frac{Q}{RT}\right) \tag{4}$$

Then, Q can be expressed as

$$Q = R\left[\frac{\partial \ln\sinh(\alpha\sigma)}{\partial(1/T)}\right]_{\dot{\varepsilon}}\left[\frac{\partial \ln\dot{\varepsilon}}{\partial \ln\sinh(\alpha\sigma)}\right]_{T} \tag{5}$$

In order to calculate Q, $\ln\dot{\varepsilon}$ is plotted versus $\ln[\sinh(\alpha\sigma)]$ as shown in Fig. 8 (a) and $\ln[\sinh(\alpha\sigma)]$ versus $1000/T$ is shown in Fig. 8(b). From the fitting lines in Fig. (8), the average value of Q was calculated to be 110 kJ/mol. The activation energy was quite close to the value for self-diffusion (Q_{sd}=135 kJ/mol) [23], but this should not deceive the nature of the controlling deformation mechanism (for Q=Q_{sd} deformation should be recovery-controlled), since DRX plays a significant role indicated in microstructure analysis. The value of activation energy was influenced by temperature, strain rate and initial microstructure, therefore it is difficult to compare the results from different research. In the previous research on ZK21 alloy compressed at the same conditions, Q was reported to be 161 kJ/mol [15]. It can

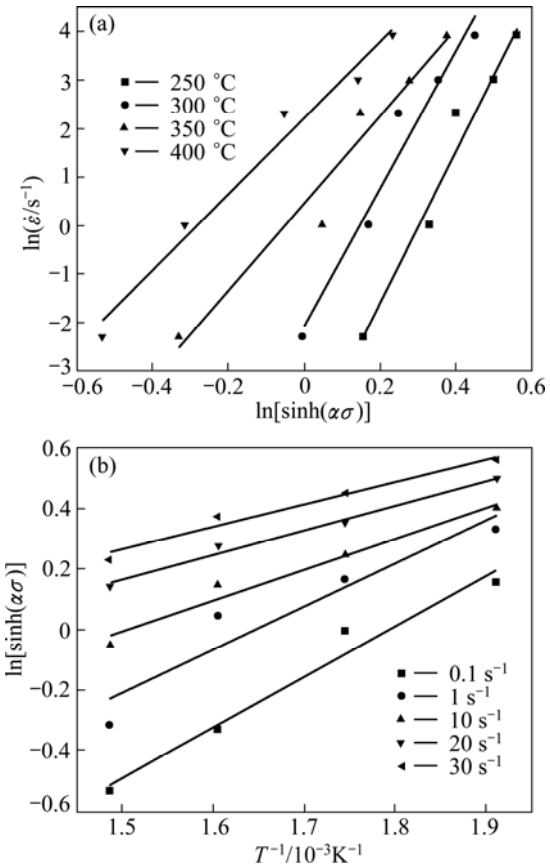

Fig. 8 Plots of $\ln[\sinh(\alpha\sigma)]-\ln\dot{\varepsilon}$ (a) and $\ln[\sinh(\alpha\sigma)]-1/T$ (b)

be found that the activation energy Q decreased with the increased Zn content in ZK series magnesium alloys, which was opposite to AZ series alloys reported in Ref. [24].

By substituting the calculated values of α and Q into Eq. (3), the relationship between $\ln[\sinh(\alpha\sigma)]$ and $\ln Z$ is plotted in Fig. 9. From the slope of the fitting line, the exponential coefficient n was calculated to be 9.7 and thus Eq. (3) could be written as follows:

$$\dot{\varepsilon} = 4.18\times10^{9}[\sinh(\alpha\sigma)]^{9.7}\exp[-110000/(RT)] \tag{6}$$

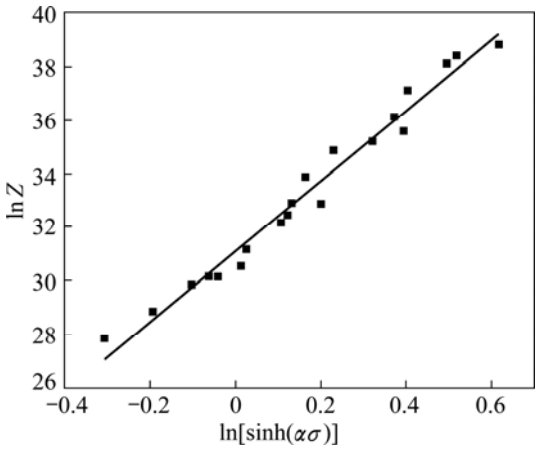

Fig. 9 Arrhenius plot of $\ln Z$−$\ln[\sinh(\alpha\sigma)]$ of ZK60 alloy during hot compression

4 Conclusions

1) At lower strain rate (0.1−1 s^{-1}), DRX developed mainly at the grain boundaries. Meanwhile, at higher strain rate (10−50 s^{-1}), DRX extensively developed at the grain boundaries and twins, resulting in a more homogeneous microstructure.

2) The optimum hot processing parameters for ZK60 alloys were strain rate of 10−50 s^{-1} and deformation temperature of 250−350 °C.

3) The evolution of twin induced DRX developed at high-strain rate compression can be divided into three stages. Firstly, twins with high dislocation density subdivided the initial grain, then dislocation arrays subdivided the twins into subgrains, and after that DRX took place with a further increase in strain.

4) The activation energy Q and stress exponent n for ZK60 alloys were deduced to be 110 kJ/mol and 9.7 by constitutive analysis.

References

[1] AVEDSIAN M M, BAKER H. ASM specialty handbook: Magnesium and magnesium alloys [M]. Materials Park: ASM International, 1999: 1−11.

[2] WU D, TANG W N, CHEN R S, HAN H E. Strength enhancement of Mg−3Gd−1Zn alloy by cold rolling [J]. Transactions of Nonferrous Metals Society of China, 2013, 23: 301−306.

[3] WU Y Z, YAN H G, CHEN J H, ZHU S Q, SU B, ZENG P L. Microstructure and mechanical properties of ZK60 magnesium alloy fabricated by high strain rate multiple forging [J]. Materials Science and Technology, 2013, 29(1): 54−59.

[4] TANG W Q, HUANG S Y, ZHANG S R, LI D Y, PENG Y H. Influence of extrusion parameters on grain size and texture distributions of AZ31 alloy [J]. Journal of Materials Processing Technology, 2011, 211(7): 1203−1209.

[5] YU Z H, YAN H G, YIN X Y, LI Y, YAN G H. Liquation cracking in laser beam welded joint of ZK60 magnesium alloy [J]. Transactions of Nonferrous Metals Society of China, 2012, 22: 2891−2897.

[6] YU Z H, YAN H G, CHEN S J, CHEN J H, ZENG P L. Method for welding highly crack susceptible magnesium alloy ZK60 [J]. Science and Technology of Welding and Joining, 2010, 15(5): 354−360.

[7] YU H, YU H S, KIM Y M, YOU B S, MIN G H. Hot deformation behavior and process maps of Mg−Zn−Cu−Zr magnesium alloy [J]. Transactions of Nonferrous Metals Society of China, 2013, 23: 756−764.

[8] GALIYEV A, KAIBYSHEV R, GOTTSTEIN G. Correlation of plastic deformation and dynamic recrystallization in magnesium alloy ZK60 [J]. Acta Materialia, 2001, 49(7): 1199−1207.

[9] GALIYEV A, SITDIKOV O, KAIBYSHEV R. Deformation behavior and controlling mechanisms for plastic flow of magnesium and magnesium alloy [J]. Materials Transactions, 2003, 44(4): 426−435.

[10] YANG Y Q, LI B C, ZHANG Z M. Flow stress of wrought magnesium alloys during hot compression deformation at medium and high temperatures [J]. Materials Science and Engineering A, 2009, 499(1−2): 238−241.

[11] HE Y B, PAN Q L, CHEN Q, ZHANG Z Y, LIU X Y, LI W B. Modeling of strain hardening and dynamic recrystallization of ZK60 magnesium alloy during hot deformation [J]. Transactions of Nonferrous Metals Society of China, 2012, 22: 246−254.

[12] WANG C Y, WU K, ZHENG M Y. Hot deformation behavior and processing map of squeeze cast ZK60 magnesium [J]. Transactions of Nonferrous Metals Society of China, 2006, 16: 1758−1761.

[13] LIU Z Y, DUAN A J, HOU Y H, KANG S, CHO J. Microstructure evolution and flow behavior during hot compression of twin roll cast ZK60 magnesium alloy [J]. Materials Science and Technology, 2010, 26(12): 1429−1438.

[14] LI L X, LOU Y, YANG L B, PENG D S, RAO K P. Flow stress behavior and deformation of Ti−3Al−5V−5Mo compressed at elevated temperatures [J]. Materials Design, 2002, 23(5): 451−457.

[15] WU Y Z, YAN H G, CHEN J H, ZHU S Q, LIU Z W, TIAN J. Hot deformation behavior and microstructure evolution of ZK21 magnesium [J]. Materials Science and Engineering A, 2010, 527(16−17): 3670−3675.

[16] GUO Q, YAN H G, CHEN Z H, ZHANG H. Elevated temperature compression behavior of Mg−Al−Zn alloys [J]. Materials Science and Technology, 2006, 22(6): 725−729.

[17] SPIGARELLI S, MEHTEDI M E, CABIBBO M, EVANGELISTA E, KANEKO J, JAGER A, GARTNEROVA V. Analysis of high-temperature deformation and microstructure of an AZ31 magnesium alloy [J]. Materials Science and Engineering A, 2007, 462(1−2): 197−201.

[18] LIU J W, CHEN Z H, CHEN D, LI G F. Deformation mechanism and softening effect of extruded AZ31 magnesium alloy sheet at moderate temperatures [J]. Transactions of Nonferrous Metals Society of China, 2012, 22: 1329−1335.

[19] YAN H G, WU Y Z, CHEN J H, ZHU S Q, SU B, ZENG P L. Microstructure evolution of ZK40 magnesium alloy during high strain rate compression deformation at elevated temperatures [J]. Materials Science and Technology, 2011, 27(9): 1416−1421.

[20] WANG K L, LU S Q, FU M W, LI X, DONG X J. Optimization of β/near-β forging process parameters of Ti−6.5Al−3.5Mo−1.5Zr−0.3Si by using processing maps [J]. Materials Characterization, 2009, 60(6): 492−498.

[21] SUN H Q, SHI Y N, ZHANG M X, LU K. Plastic strain-induced grain refinement in the nanometer scale in a Mg alloy [J]. Acta Materialia, 2007, 55(3): 975−982.

[22] McQUEEN H J, RYAN N D. Constitutive analysis in hot working [J]. Materials Science and Engineering A, 2002, 322(1−2): 43−63.

[23] MOREAU G, COMET J A, CALAIS D. Acceleration of the chemical diffusion under irradiation in the system aluminium-magnesium [J]. Journal of Nuclear Materials, 1971, 38(2): 197−202.

[24] LIU L F, DING H L. Study of the plastic flow behaviors of AZ91 magnesium alloy during thermomechanical process [J]. Journal of Alloys and Compounds, 2009, 484(1−2): 949−956.

ZK60 镁合金高应变速率压缩变形的流变行为及显微组织

吴远志[1,2]，严红革[3]，朱素琴[4]，陈吉华[3]，刘安民[1,2]，刘先兰[1]

1. 湖南工学院 机械工程学院，衡阳 421002；
2. 湖南工学院 先进制造技术研究所，衡阳 421002；
3. 湖南大学 材料科学与工程学院，长沙 410082；
4. School of Aerospace, Mechanical & Mechatronic Engineering, The University of Sydney, Sydney NSW 2006, Australia

摘 要：在 250~400 °C 的温度范围和 0.1−50 s^{-1} 的应变速率范围内对 ZK60 合金进行压缩变形，对其流变行为和显微组织进行研究。结果表明，在低应变速率(0.1~1 s^{-1})下压缩变形时，再结晶主要发生在初始晶界上；在高应变速率(10~50 s^{-1})下压缩变形时，再结晶同时在初始晶界和孪晶上发生。合金在应变速率 10~50 s^{-1} 和温度 250~350 °C 的变形条件下获得均匀、细小的再结晶组织。因此，合金的最佳热加工工艺范围为应变速率 10~50 s^{-1}、变形温度 250~350 °C。高应变速率压缩变形条件下的孪生诱发动态再结晶过程分三步，首先，高位错密度孪晶分割初始晶粒；然后，孪晶内的位错发生重排形成亚晶；最后，随着应变的增加而形成再结晶晶粒。

关键词：ZK60 镁合金；高应变速率压缩；流变行为；显微组织；孪生诱发动态再结晶

(Edited by Hua YANG)